Toxicology and Applied Pharmacology 475 (2023) 116650

Contents lists available at ScienceDirect

Toxicology and Applied Pharmacology

journal homepage: www.elsevier.com/locate/taap

A comparative proteomics analysis of four contact allergens in THP-1 cells shows distinct alterations in key metabolic pathways

Tessa Höper [a,b,1], Isabel Karkossa [c,1], Verónica I. Dumit [a], Martin von Bergen [c,d,e], Kristin Schubert [c], Andrea Haase [a,*]

[a] Department of Chemical and Product Safety, German Federal Institute for Risk Assessment (BfR), Berlin, Germany
[b] Department of Clinical Pharmacy and Biochemistry, Institute of Pharmacy, Freie Universität Berlin, Berlin, Germany
[c] Department of Molecular Systems Biology, UFZ, Helmholtz-Centre for Environmental Research, Leipzig, Germany
[d] Institute of Biochemistry, Leipzig University, Leipzig, Germany
[e] German Centre for Integrative Biodiversity Research (iDiv) Halle-Jena-Leipzig, Leipzig, Germany

ARTICLE INFO

Editor: Lawrence Lash

Keywords:
Allergic contact dermatitis
Proteomics
THP-1 cells
Monocyte-derived dendritic cells
SILAC
LFQ

ABSTRACT

Allergic contact dermatitis (ACD) is the predominant form of immunotoxicity in humans. The sensitizing potential of chemicals can be assessed *in vitro*. However, a better mechanistic understanding could improve the current OECD-validated test battery. The aim of this study was to get insights into toxicity mechanisms of four contact allergens, *p*-benzoquinone (BQ), 2,4-dinitrochlorobenzene (DNCB), *p*-nitrobenzyl bromide (NBB) and $NiSO_4$, by analyzing differential proteome alterations in THP-1 cells using two common proteomics workflows, stable isotope labeling by amino acids in cell culture (SILAC) and label-free quantification (LFQ). Here, SILAC was found to deliver more robust results. Overall, the four allergens induced similar responses in THP-1 cells, which underwent profound metabolic reprogramming, including a striking upregulation of the TCA cycle accompanied by pronounced induction of the Nrf2 oxidative stress response pathway. The magnitude of induction varied between the allergens with DNCB and NBB being most potent. A considerable overlap between transcriptome-based signatures of the GARD assay and the proteins identified in our study was found. When comparing the results of this study to a previous proteomics study in human primary monocyte-derived dendritic cells, we found a rather low share in regulated proteins. However, on pathway level, the overlap was high, indicating that affected pathways rather than single proteins are more eligible to investigate proteomic changes induced by contact allergens. Overall, this study confirms the potential of proteomics to obtain a profound mechanistic understanding, which may help improving existing *in vitro* assays for skin sensitization.

1. Introduction

Developing alternative testing strategies for chemical safety testing has been an overarching topic in regulatory toxicology for decades. The strict ban on animal testing for cosmetic ingredients in the European Union (EC, 2009) has led to great advances in this field. For simple toxicological endpoints, such as skin irritation or skin corrosion, several test guidelines accepted by the Organization for Economic Co-operation and Development (OECD) have been available for a long time. The more complex endpoints like skin sensitization remained challenging as multiple key events had to be identified and covered by test systems. The Adverse Outcome Pathway (AOP) that the OECD published for skin

Abbreviations: ACLY, ATP-citrate synthase; ACN, acetonitrile; AOP, adverse outcome pathway; BIN2, bridging integrator 2; BQ, p-benzoquinone; COX, cytochrome *c* oxidase; DC, dendritic cell; DMSO, dimethyl sulfoxide; DNAAJA, DnaJ homolog subfamily A member; DNAJC, DnaJ homolog subfamily C member; DNCB, 2,4-dinitrochlorobenzene; EPHX, epoxide hydrolase; FC, fold change; GARD, Genomic Allergen Rapid Detection; GCLM, glutamate-cysteine ligase; GSR, glutathione reductase; h-CLAT, human Cell Line Activation Test; HMGCS, hydroxymethylglutaryl-CoA synthase; IDH, isocitrate dehydrogenase; KE, key event; LFQ, label-free quantification; MGST, microsomal glutathione S-transferase; NBB, p-nitrobenzyl bromide; NDUF, NADH dehydrogenase; Ni, NiSO4; NQO, NAD(*P*)H dehydrogenase (quinone); OXPHOS, oxidative phosphorylation; PCA, principal component analysis; PPP, pentose phosphate pathway; SOD, superoxide dismutase; SUCNR, succinate receptor 1; TOMM40, mitochondrial import receptor subunit TOM40 homolog; TXNRD, thioredoxin reductase; WO, with out.

* Corresponding author.
E-mail address: andrea.haase@bfr.bund.de (A. Haase).
[1] These authors have contributed equally to this work.

https://doi.org/10.1016/j.taap.2023.116650
Received 27 April 2023; Received in revised form 21 July 2023; Accepted 31 July 2023
Available online 3 August 2023

sensitization in 2012 (OECD, 2014) paved the way for several alternative test methods, each addressing key events (KEs) of the AOP, ultimately leading to the Defined Approach released by OECD in 2021 (OECD, 2021). The skin sensitization AOP starts from the haptenation of allergens with proteins in the skin as the molecular initiating event, which can be assessed *in chemico* using the direct peptide reactivity assay (Gerberick et al., 2004; OECD, 2022a). The next KEs are the cellular activation of keratinocytes and dendritic cells (DC), which can be evaluated *in vitro* (OECD, 2022b, 2022c). The KeratinoSens™ is validated for estimating keratinocyte activation based on the gene expression of the antioxidant response element as well as Nrf2 (Emter et al., 2010; OECD, 2022b), and activation of DCs can be determined based on the expression of selected cell surface proteins. The human cell line activation test (hCLAT) for example utilizes upregulation of CD54 and CD86 on THP-1 cells as a measure for DC activation after exposure to sensitizing chemicals (Ashikaga et al., 2006; OECD, 2022c). Activated DCs then migrate to the lymph nodes, where they present the hapten to naïve T cells, inducing their activation and proliferation. T cell proliferation in the lymph nodes was recognized in the AOP as the organ response. However, to date no validated alternative test method for the assessment of T cell activation exists.

Despite these substantial achievements, the currently available alternative test methods for skin sensitization have several limitations. For example, pre- and prohaptens are difficult to predict since some test systems lack the metabolic competency to convert the chemicals into their reactive metabolite. For instance, *in chemico* methods like the direct peptide reactivity assay entirely lack metabolic activity and also cell-based test systems like the hCLAT were shown to have limitations regarding metabolic activation of substances (Gerberick et al., 2004; Ashikaga et al., 2010; Fabian et al., 2013; Oesch et al., 2014). Also, most assays are not designed for the testing of lipophilic compounds (Gerberick et al., 2007; Ashikaga et al., 2010; Takenouchi et al., 2013). Furthermore, the accurate potency classification of sensitizers is not yet fully resolved (Nukada et al., 2013; Jaworska et al., 2015; Reisinger et al., 2015). Thus, further work is needed. In particular a more detailed mechanistic understanding can be helpful, as the current methods provide only very limited insights into the underlying modes of action. For this purpose, omics approaches are especially well suited as they deliver comprehensive mechanistic insights. To date, mostly transcriptomics was used to characterize cellular changes induced by contact allergens in patient's biopsies as well as *in vitro* (Johansson et al., 2011; Dhingra et al., 2014; Lefevre et al., 2021), which also led to the development of the GARD (Genomic Allergen Rapid Detection) assay. The GARD assay comprises a signature of 200 transcripts that allows to discriminate between contact allergens and non-allergens (Johansson et al., 2013). The identity of the discriminating genes is disclosed but further information (*e.g.* direction of regulation) has not been published. Recently, the GARD assay underwent official validation and became an OECD test guideline for skin sensitization (OECD, 2022c). In contrast to transcriptomics, the potential of proteomics has not been fully exploited, yet. Proteomics is typically applied to identify cellular haptenation sites (Parkinson et al., 2014; Guedes et al., 2016; Parkinson et al., 2018; Parkinson et al., 2020), while proteomic studies that aim to unravel cellular changes in allergen-treated DCs remain scarce (as reviewed by Höper et al., 2017). DCs play a major role during skin sensitization as they act as link between adaptive and innate immune system and thereby commence the cell-mediated allergic immune response. Exposure of DCs to contact allergens induces maturation accompanied by reconstruction of the cell organelles and membranes. Upregulation of protein expression serves the elevated energy demand necessary for maturation as well as the crosstalk with other immune cells, particularly T cells. Hence, our aim was to conduct a comprehensive proteomic study to unravel regulated proteins. For this purpose, we selected THP-1 cells, since this is the utilized cell model in the OECD-validated hCLAT assay. THP-1 cells were treated with the four contact allergens, *p*-benzoquinone (BQ), 2,4-dinitrochlorobenzene (DNCB), *p*-nitrobenzyl bromide (NBB) and $NiSO_4$ (Ni) to assess whether the different allergens induce similar proteins and pathways in the cells, which could potentially be used as a predictive protein-based signature for skin sensitization. As we expected that potent allergens most likely induce more alterations compared to moderate or weak allergens, we intentionally selected DNCB, BQ and NBB, which have been classified as extreme sensitizers in the LLNA (Gerberick et al., 2005). The potency of nickel salts is ranked as weak to moderate, yet nickel is the most prevalent allergen in the EU (Oosterhaven et al., 2019). In addition, nickel appeared relevant to us as, in contrast to other allergens, it can directly interact with and bind to the TLR4 and, therefore, does not rely on indirect receptor activation (Martin et al., 2011). Furthermore, we applied and compared two common proteomic quantification approaches, SILAC (stable isotope labeling by amino acids in cell culture) and LFQ (label-free quantification). SILAC is a very common approach for cell cultures and is considered a very robust quantification technique (Li et al., 2012). LFQ was included as it is frequently used due to its wide range of applications. Moreover, we used this approach in our previous proteomics study in primary human dendritic cells (Höper et al., 2021). As debates in the scientific community are still ongoing whether THP-1 cells are a good model to properly mimic responses of DCs, we also compared the proteomic data derived from this study to the ones obtained in primary human DCs earlier (Höper et al., 2021).

2. Material and methods

Unless otherwise stated, all chemicals were purchased from Sigma-Aldrich. Phosphate buffered saline (PBS, P04–36500), RPMI 1640 (P04–17500), HEPES (P05–01100), sodium pyruvate (P04–43100), L-glutamine (P04–80100) and penicillin-streptomycin (P06–07100) were purchased from PAN.

2.1. Cell culture

THP-1 cells were purchased from Leibniz Institute DSMZ-German Collection of Microorganisms and Cell Cultures (Braunschweig, Germany). Cells were grown in RPMI 1640 media supplemented with 10% (*v*/v) fetal bovine serum (Merck, S0615), 10 mM HEPES, 2 mM L-glutamine (2 mM), sodium pyruvate (1 mM) and penicillin/streptomycin (100 U/ml) at 37 °C in an incubator with 5% CO_2. Every 3 to 4 days, cells were passaged and seeded at 1×10^5 cells per ml in T75 flasks.

2.2. Cell culture for SILAC experiments

For SILAC experiments, cells were grown in SILAC RPMI media (Thermo Fisher Scientific, A33823) supplemented with 10% (*v*/v) dialyzed fetal bovine serum (Thermo Fisher Scientific, 26400044) and isotope labeled amino acids. Medium control cells were grown in medium containing $^{13}C_6$-L-lysine (Silantes, 211204102) and $^{13}C_6$-L-arginine (Silantes, 201204102). Chemical-treated cells as well as vehicle controls were cultured in medium containing the light amino acids $^{12}C_6$-L-lysine (Silantes, 211003902) and $^{12}C_6$-L-arginine (Silantes, 201004102), respectively. Complete incorporation of the amino acids after 7 days was verified beforehand and cells were treated as mentioned below.

2.3. Chemical treatment

Cells were seeded in 6-well plates with a density of 1×10^6 cells per well and immediately treated for 24 h with 400 μM Ni (31483), 20 μM BQ (B10358), 10 μM DNCB (237329) or 2 μM NBB (N13054). The metal allergen Ni was dissolved in cell culture medium, whereas the other organic allergens were dissolved in dimethyl sulfoxide (DMSO, Merck, D2438). The stock solutions were diluted in medium and the final DMSO concentration in the cell suspension was <0.2% (*v*/v). DMSO

concentrations were in accordance with maximum levels allowed in OECD TG 442 E (OECD, 2022c). Medium-only treated cells were included as control and DMSO-treated cells were used as vehicle controls.

2.4. Viability assessment

Cell viability was assessed by flow cytometry. Cells were harvested, centrifuged (5 min, 300 xg, RT) and washed with PBS. Staining for flow cytometry was performed for 30 min at 4 °C using fixable near-IR dead cell stain (Thermo Fisher Scientific, L34976). Data were acquired using a FACSAria III flow cytometer (BD Biosciences) and analyzed with FlowJo software (V.10.7.1, FlowJo LLC, Ashland, OR, United States).

2.5. Proteome analysis

2.5.1. Cell harvest and lysis

After 24 h of treatment, cells were harvested by centrifugation (5 min, 300 xg, RT). Cell pellets were washed twice with ice-cold PBS, and the washed cells were lysed in 100 µl lysis buffer per 10^6 cells. The lysis buffer was composed of 150 mM NaCl (S7653-250G), 10 mM TRIS pH 7.2 (T1503-250G), 5 mM EDTA (E5134-250G), 0.1% (*v*/v) SDS (436143-25G), 1% (v/v) Triton X-100 (T8787-100ML), 1% (v/v) sodium deoxycholate (30970-100G), 200 µM phenylmethylsulfonyl fluoride (P7626-1G), 1 mM sodium orthovanadate (S6508-10G) and cOmplete protease inhibitor cocktail (Roche, 1.167.498.001). Cells were thoroughly vortexed, incubated on ice for 15 min and sonicated to shear DNA. Subsequently, the samples were centrifuged (10 min, 16,000 g, 4 °C), and the supernatant was collected. The protein concentration of the supernatant was determined using Pierce BCA protein assay (Thermo Fisher Scientific, 23225). For SILAC experiments, equal protein numbers of treated and control cells were combined in a fresh tube.

2.5.2. Sample preparation

For each sample condition, 30 µg protein were diluted in 100 mM triethylammonium bicarbonate buffer (T7408). Proteins were reduced using 200 mM tris(2-carboxyethyl)phosphine (Serva, 36970.01) and subsequently alkylated with 375 mM iodoacetamide (Serva, 26710.02). For tryptic digestion of the proteins, the lysis buffer was removed using SpeedBeads™ magnetic carboxylate modified particles (SP3 beads, GE Healthcare, 65152105050250). Organic concentration of the samples was adjusted to >50% (*v*/v) acetonitrile (ACN, 1000292500) to enable binding of the proteins to the beads. The beads were washed twice with 70% (*v*/v) ethanol (1117272500) and once with ACN. Proteins were digested using trypsin (1:50 ratio, Promega, V5117) in 50 mM ammonium bicarbonate buffer. After tryptic digestion, the aqueous supernatant containing the peptides was collected and transferred to a fresh tube. The beads were washed with 50 mM ammonium bicarbonate and the supernatant was collected into the same tube as before. Peptides were then prepared for LC-MS analysis using solid phase extraction cartridges (Waters, 186000383), vacuum-dried and reconstituted in 0.1% (*v*/v) formic acid (00940) prior to measurement.

2.5.3. LC-MS/MS

An UPLC system (Ultimate 3000, Dionex, Thermo Fisher Scientific) coupled to a Q Exactive HF (Thermo Fisher Scientific) was used to analyze the samples as described previously for LFQ (Wang et al., 2020). Peptides were injected to an Acclaim PepMap 100 C18 trap column (3 µm, nanoViper, 75 µm × 5 cm, Thermo Fisher Scientific, PN164535) at a flow rate of 5 µl/min using a loading eluent composed of 2% (v/v) ACN and 0.05% (v/v) trifluoroacetic acid (Biosolve, 202341A8) in water. Peptides were subsequently separated by a 150 min non-linear gradient from 0 to 80% (v/v) ACN in 0.1% (v/v) formic acid on a reversed-phase column (Acclaim PepMap 100 C18, 3 µm, nanoViper, 75 µm × 25 cm, Thermo Fisher Scientific, PN164569). Ionization was performed with a chip-based ESI source (Nanomate, Advion, Ithaca, NY, United States). The MS1 scans were acquired at a resolution of 120 K in a range of 350–1550 *m/z*. AGC target was set to 3×10^6 with a maximal injection time of 10 ms. MS2 data acquisition was based on a Top 10 approach with an isolation window of 1.4 *m/z*. Peptides were fragmented at normalized collision energy of 28, and the fragment ion spectra were acquired at a resolution of 15 K using AGC target of 2×10^5 and maximal IT of 100 ms. Dynamic exclusion was set to 20 s. All spectra were acquired using XCalibur (Version 4.2).

2.5.4. Data analysis

MaxQuant Version 1.6.2.10 (Cox et al., 2014) was used to process the raw MS data using the default parameters if not indicated otherwise. For peptide identification, a database search against the *Homo sapiens* UniProtKB reference proteome (07-10-2021) was performed. Carbamidomethylation of cysteine was set as fixed, whereas oxidation of methionine and acetylation of protein N-terminus were set as variable modifications. Protein identification was performed applying a false discovery rate ≤ 0.01 to proteins, with a minimum of two peptides and at least one unique peptide. The protein quantification was performed on the basis of two unique peptides. Match between runs was activated. Protein contaminants, identification only by site and reverse hits were excluded before further use. SILAC and LFQ protein intensities were processed, and results were visualized in R-3.5.0 using the following packages: plyr (Wickham, 2011), reshape2 (Wickham, 2007), xlsx (Adrian and Cole, 2018), DEP (Zhang et al., 2018), mixOmics (Rohart et al., 2017), pheatmap (Kolde, 2019), ggsci (Nan, 2018), circlize (Gu, 2014), calibrate (Jan, 2019), ggplot2 (Hadley, 2016), dendsort (Sakai, 2015), readxl (Hadley and Jennifer, 2019), qpcR (Andrej-Nikolai, 2018), splitstackshape (Ananda, 2019), tidyr (Hadley and Lionel, 2019), and Tmisc (Stephen, 2019) Accordingly, the data were Log2-transformed, filtered for proteins that were quantified in a minimum of three replicates under at least one condition, followed by variance-stabilization. Fold changes (FCs) were calculated relative to medium control. For SILAC, p-values were calculated using Student's *t*-test based on the Log2(FC) of the replicates tested against 0. For LFQ samples, p-values were calculated relative to medium control replicates. P-values were adjusted according to Benjamini and Hochberg. Proteins with an adjusted p-value ≤0.05 were considered regulated.

2.5.5. Pathway enrichment

Enriched pathways were identified using Ingenuity Pathway Analysis (IPA) (Qiagen, 2023; Krämer et al., 2013), considering regulated proteins (adjusted p-value ≤0.05). For this purpose, the database was filtered for human data, and the tissue specificity was set to immune cells. Obtained z-scores reflect the regulation direction and Benjamini and Hochberg adjusted p-values indicate significance of enrichment. Pathways were considered significantly enriched with adjusted p-value ≤0.05.

3. Results

3.1. SILAC quantification outperforms LFQ with respect to the number of regulated proteins

The aim of this study was to obtain novel insights into proteomic changes during cellular activation of contact allergen-treated THP-1 cells exposed to 20 µM BQ, 10 µM DNCB, 2 µM NBB or 400 µM Ni for 24 h. Cell viability was ensured to be at least 75% (Supplementary Fig. 1), in concordance with the CV75 value of the h-CLAT assay (OECD, 2022c). First, we compared two untargeted proteomics approaches, SILAC and LFQ, regarding their potential to identify regulated proteins.

Overall, 1997 and 2200 proteins were reliably quantified using SILAC and LFQ, respectively, of which 1904 proteins were identified by both methods (Fig. 1A). A principal component analysis (PCA) of SILAC-quantified proteins revealed that proteomic changes induced by the contact allergens DNCB and NBB led to a clear separation from vehicle

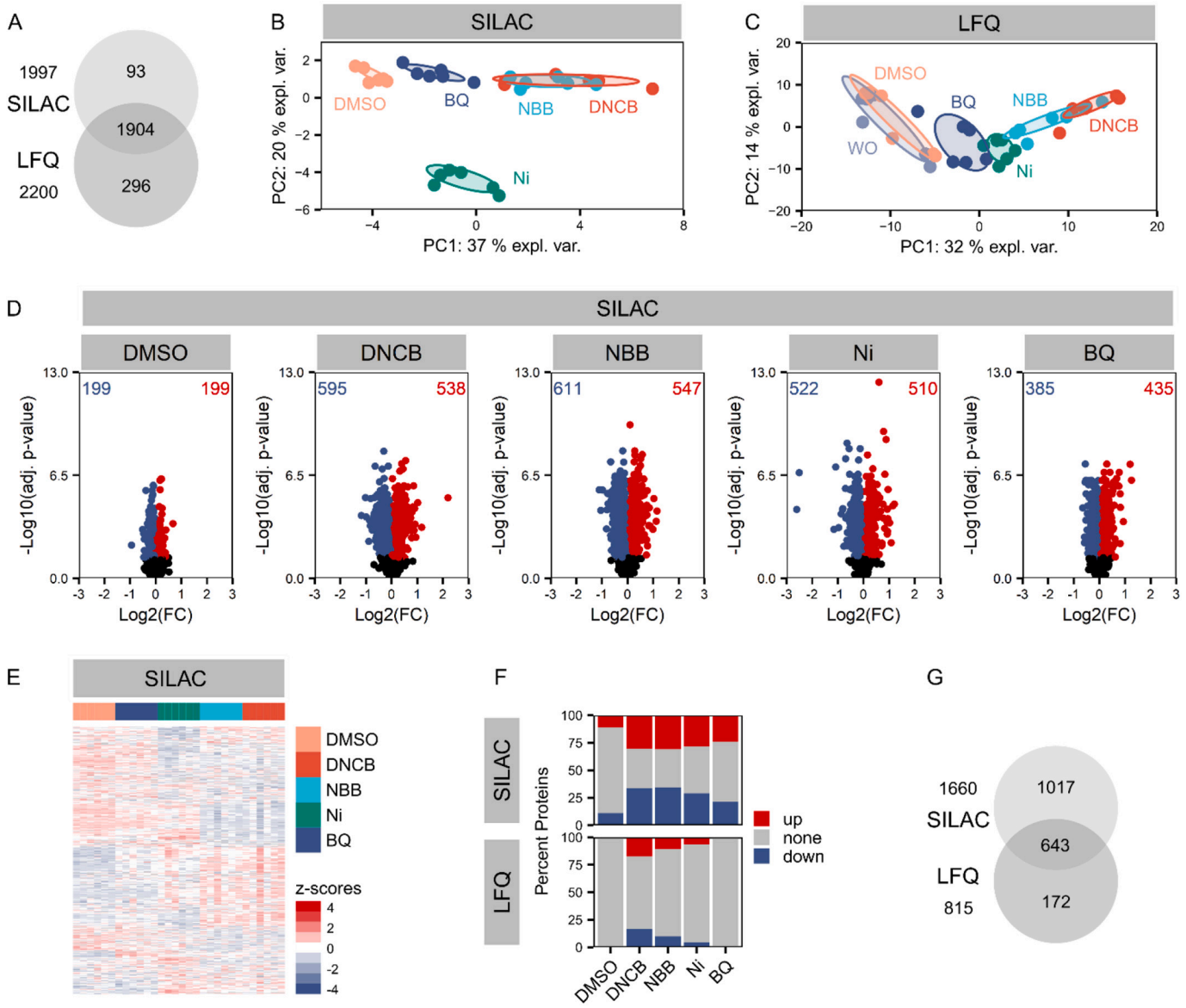

Fig. 1. Quantitative proteomic analysis in THP-1 cells treated with skin sensitizers. THP-1 cells were treated with the allergens BQ, DNCB, NBB or Ni. DMSO (solvent control) and medium only (WO) samples were used as controls. The number of quantified proteins is displayed in (A). PCA revealed general differences between treated cells and controls for SILAC (B) and LFQ (C) data. Volcano plots showing Log2(FCs) and –Log10(adjusted p-values) of allergen-treated THP-1 cells indicated changes induced by the allergens tested here. Numbers of regulated proteins (adjusted p-value ≤0.05; up: Log2(FC) > 0, red; down: Log2(FC) < 0, blue) are provided in the corners (D). Clustering of regulated proteins was determined using z-scored replicate data (E). Percentages of regulated proteins were compared for SILAC and LFQ data (F). Regulated proteins shared between SILAC and LFQ data were determined (G). (For interpretation of the references to colour in this figure legend, the reader is referred to the web version of this article.)

controls (DMSO). Separation of Ni-treated cells from controls and other treatments was distinct (Fig. 1B). LFQ also resulted in a separation of the allergens DNCB, NBB and Ni from controls. BQ-treated cells clustered in between. Overall, separation of the different treatments was not as clear compared to SILAC quantification (Fig. 1C). Next, regulated proteins (adjusted p-value ≤0.05) were determined, and comparing the distribution of Log2(FCs) and -Log10(adjusted p-values) for SILAC (Fig. 1D) and LFQ data (Supplementary Fig. 2A), it was noted that Log2(FC) ranges were smaller in SILAC data than in LFQ data. Notably, a high reproducibility and treatment-specific cluster formation of regulated proteins was observable with both methods (SILAC: Fig. 1E, LFQ: Supplementary Fig. 2B). Again, DNCB- and NBB-induced clusters differed clearly from control cells, whereas BQ-induced proteins predominantly clustered with control cells. Ni-treatment induced clusters that differed from controls as well as the other treatments. Interestingly, when comparing the numbers of regulated proteins, we found that SILAC resulted in a higher percentage for each treatment (Fig. 1F) and also a higher number of regulated proteins in at least one treatment than LFQ (Fig. 1G). Although 643 proteins were regulated in both SILAC and LFQ data, the majority of regulated proteins (1017) were identified exclusively in SILAC data (Fig. 1G).

Overall, the allergens clearly induced effects, which were detectable using SILAC and LFQ. Since SILAC yielded more regulated proteins (Fig. 1G) and showed a clearer separation of treatments (Fig. 1B), we decided to focus on SILAC data for subsequent analyses. Nevertheless, corresponding LFQ results are available in the supplementary material.

3.2. Contact allergen-exposed THP-1 cells show pronounced metabolic reprogramming

Next, an IPA pathway analysis was employed for regulated proteins (adjusted p-value ≤0.05) to gain functional insights into the effects of contact allergens on the pathway level. The majority of the significantly (adjusted p-value ≤0.05) enriched IPA pathways (74) was shared for SILAC and LFQ but again SILAC outperformed LFQ as more pathways were found significantly enriched (Fig. 2A). Among the TOP 30 significantly enriched pathways identified using SILAC, most pathways were regulated uniformly by the four allergens tested (Fig. 2B). The magnitude of induction varied with DNCB and NBB being the most potent inducers of cellular response mechanisms. Interestingly, five pathways were directly related to cellular metabolism: Oxidative phosphorylation (OXPHOS), gluconeogenesis, TCA cycle and pentose phosphate pathway were upregulated, pointing towards an increased cellular energy demand. β-oxidation of fatty acids was significantly upregulated after treatment with DNCB, NBB and Ni but was downregulated in BQ-treated cells (Fig. 2B). Of these pathways, OXPHOS was strongly upregulated after contact allergen exposure of the THP-1 cells (Fig. 2B). OXPHOS serves to supply the cell with ATP produced by a series of five protein complexes in the inner mitochondrial membrane. Several isoforms and subunits of the enzymes belonging to the electron transport chain were found to be upregulated, including NADH dehydrogenase (NDUF, complex I), cytochrome *c* oxidase (COX, complex IV) and ATP synthase (ATP, complex V) (Fig. 2C). Furthermore, the TCA cycle was highly affected (Fig. 2B). The conversion of isocitrate to α-ketoglutarate is the rate-limiting step of the TCA cycle and is catalyzed by the enzyme isocitrate dehydrogenase (IDH). Here, we identified two subunits of IDH (IDH3A and B) to be upregulated after treatment with DNCB and NBB.

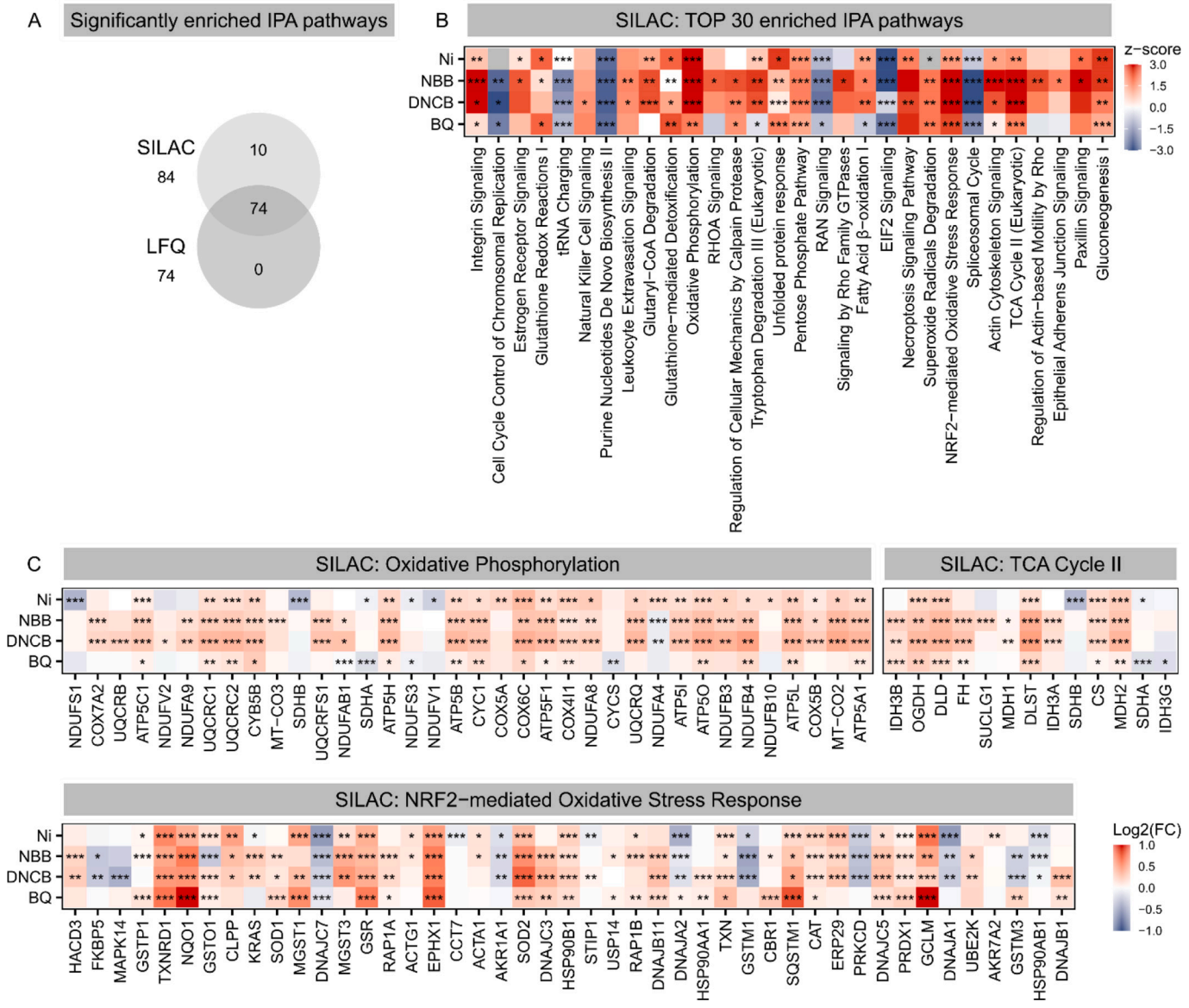

Fig. 2. Significantly enriched IPA pathways and regulated proteins assigned to selected pathways. Regulated proteins (adjusted p-value ≤0.05) were subjected to the enrichment of canonical pathways using IPA, resulting in adjusted p-values describing the significance of the enrichment and z-scores reflecting the direction of the regulation (activation (red): z-score > 0, inhibition (blue): z-score < 0). Overlaps of significantly enriched pathways (adjusted p-value ≤0.05) were compared for SILAC and LFQ data (A). TOP 30 pathways were extracted based on the adjusted p-values across all treatments for SILAC data (B). SILAC-based regulated proteins were depicted for oxidative phosphorylation, TCA cycle II and Nrf2-mediated oxidative stress response (C). Significances are indicated by asterisks: * adjusted p-value ≤0.05; ** adjusted p-value ≤0.01; *** adjusted p-value ≤0.001. (For interpretation of the references to colour in this figure legend, the reader is referred to the web version of this article.)

Treatment with BQ selectively led to the upregulation of IDH3B and the metal allergen Ni did not induce IDH at all. Succinate dehydrogenase was the only protein of the TCA cycle that was found to be down-regulated after treatment with BQ and Ni or remained unchanged for DNCB and NBB (Fig. 2C). This points towards a high succinate withdrawal from the cycle.

Moreover, the exposure to the contact allergens induced pronounced cellular stress, which was reflected in the induction of Nrf2-mediated oxidative stress response, superoxide radicals degradation, glutathione-mediated detoxification, glutathione redox reactions and unfolded protein response (Fig. 2B). With 44 assigned regulated proteins, Nrf2-mediated oxidative stress response seemed to be very relevant. Among the highly upregulated proteins, we found proteins like NAD(*P*)H dehydrogenase (quinone) 1 (NQO1), epoxide hydrolase 1

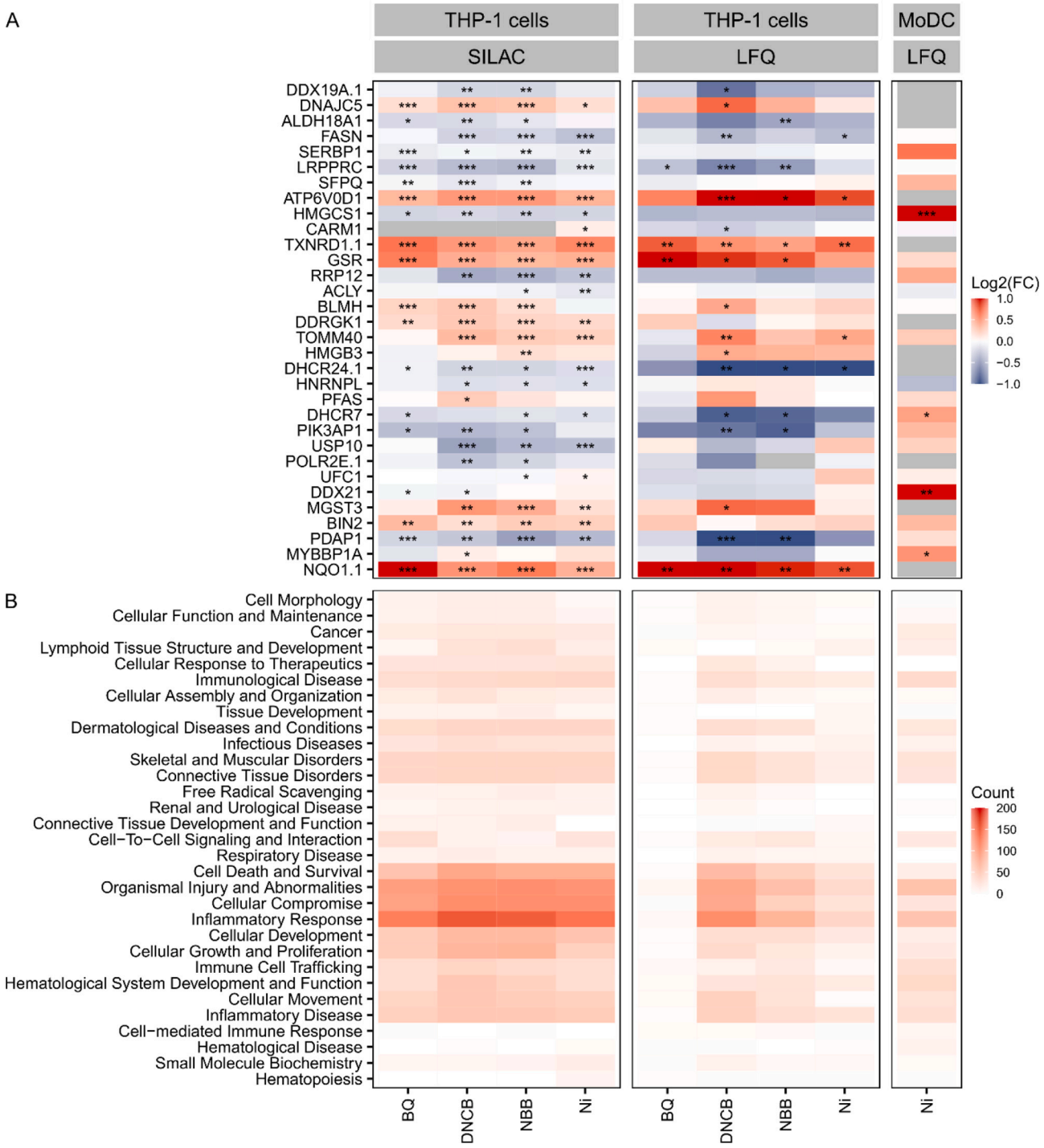

Fig. 3. Comparison of results from THP-1 cells and MoDCs. The gene signature employed by Johansson et al., 2011 to distinguish allergens from non-allergens was matched to regulated proteins in the allergen-treated THP-1 cells and the previously described MoDCs, focusing on the candidates being regulated in SILAC data. Shown are Log2(FCs) and significances for matching proteins (* adjusted p-value ≤0.05; ** adjusted p-value ≤0.01; *** adjusted p-value ≤0.001, for MoDCs, raw p-values were used) (A). According to the previously described procedure (Johansson et al. (2011)), triggered IPA diseases and biological functions were determined and filtered for those with at least 15 matching regulated proteins (adjusted p-value ≤0.05 for THP-1 cells, raw p-values ≤0.05 for MoDCs) in at least one treatment (B).

(EPHX1), thioredoxin reductase 1 (TXNRD1), superoxide dismutase 2 (SOD2), glutamate-cysteine ligase (GCLM) and glutathione reductase (GSR). The co-chaperones DnaJ homolog subfamily A member 1 (DNAJA1) and DnaJ homolog subfamily C member 7 (DNAJC7) were downregulated due to allergen treatment (Fig. 2C).

Furthermore, allergen-treatment induced downregulation of pathways involved in cell cycle maintenance and mRNA translation. Reconstruction of the actin cytoskeleton was also represented in the TOP 30 IPA pathways (Fig. 2B). Analogous figures for LFQ data are provided in the supplement (Supplementary Figs. 3 and 4).

3.3. Proteomics data reflect GARD gene signature and underline central role of Nrf2-mediated stress response as well as cholesterol biosynthesis

To assess the suitability of proteomics for detection of skin sensitizing chemicals in THP-1 cells, we compared our data to complementary data from a transcriptomic study, which defined the so-called GARD signature, a set of 200 genes that was found to be applicable to distinguish allergens from irritants and non-allergens in MUTZ-3 cells (Johansson et al., 2011). In total, 43 proteins relating to the signature genes were found in the THP-1 cells investigated here (SILAC and LFQ). For SILAC data, 38 proteins were part of the signature, of which 32 were regulated by at least one allergen. With 20 regulated proteins out of 41 assigned proteins, LFQ was again outperformed by SILAC and we thus decided to focus on the SILAC candidates as before (Fig. 3A).

Matched proteins were mostly unidirectionally regulated across the four allergens investigated here. Since directionality of transcriptional regulation was not published together with the GARD signature, comparison of regulation directionality between gene and protein level was impossible. Interestingly, the signature included proteins related to cholesterol biosynthesis, including hydroxymethylglutaryl-CoA synthase (HMGCS1) and ATP-citrate synthase (ACLY). Furthermore, proteins of the antioxidant response were successfully matched to the gene signature, *i.e.* the induced proteins NQO1, TXNRD1, microsomal glutathione S-transferase 3 (MGST3) and GSR (Fig. 3A).

We then compared the data retrieved from the THP-1 cells here to data from MoDCs. MoDCs are a frequently used *in vitro* model for DCs and are derived from human blood cells. For the comparison of THP-1 cells and MoDCs, we used our previously published proteomics data, where the effects of Ni were investigated using LFQ (Höper et al., 2021). Notably, the share of regulated proteins was rather low between THP-1 cells and MoDCs (Supplementary Fig. 5), which was also reflected by the low overlap in regulated proteins among the GARD signature genes (Fig. 3A). In total, 65 proteins of the MoDC data set were assigned to the GARD signature. However, only 14 of them were regulated after treatment with Ni. In most cases, these proteins were regulated opposite for THP-1 cells compared to MoDCs. Proteins that were found to be regulated unidirectional included GSR, bridging integrator 2 (BIN2) and mitochondrial import receptor subunit TOM40 homolog (TOMM40). These proteins are involved in oxidative stress response, cell motility and mitochondrial shuttling processes, respectively. In summary, the picture that emerges is that proteomic studies reflect the GARD signature to a limited extent. Also, the comparison of two different cell models on protein level does not yield congruent results, which was independent of the quantification method used.

3.4. Similar diseases and functions were affected in THP-1 cells compared to MoDCs

The low overlap on single protein level between THP-1 cells and MoDCs (Supplementary Fig. 5) prompted us to investigate whether this would still induce a comparable effect on enrichment level. For doing so, IPA was used to analyze diseases and functions based on regulated proteins in THP-1 cells compared to MoDC data (Fig. 3B). These provide information on superordinate toxicological functions, diseases and biological processes that are regulated and thereby provide more causal and holistic information on the organism under investigation than the analysis of canonical pathways alone. As done by Johansson et al. (2011) to determine the dominating functions of the GARD prediction signature, only diseases and functions with at least 15 matched regulated proteins were considered for this comparison. Among those, diseases and functions related to inflammation and especially inflammatory responses ranked highest (Fig. 3B). Other terms related to inflammation and cell damage, like cellular compromise and organismal injury abnormalities, were also affected after treatment with the four contact allergens investigated (Fig. 3B). This inflammatory status of the cells was accompanied by biological functions involved in the cellular adaption to these conditions like cellular development, cellular function and maintenance, cell-to-cell signaling and interaction as well as cell morphology (Fig. 3B). As expected, some of the identified diseases and functions were linked to contact allergy, such as dermatological disease and conditions and cell-mediated immune response. The comparison of these results with those previously described in MoDCs treated with Ni (Höper et al., 2021) revealed similar diseases and functions to be affected (Fig. 3B). Yet, the cellular response of the MoDCs to Ni-exposure seems to be less augmented compared to THP-1 cells (Fig. 3B).

Overall, the induced diseases and functions well reflect the cellular stress induced by allergen-treatment and point towards inflammatory signaling, which was less evident in the canonical pathway analysis. Notably, we observed the induction of the very same diseases and functions in two proteomic sets with low overlap in regulated proteins, suggesting the pathway/enrichment level to be better suited for dataset comparison than the single protein level.

4. Discussion

4.1. SILAC outperforms LFQ in terms of regulated proteins and enriched pathways

The determination of the skin-sensitizing potential of chemicals is essential for proper chemical safety assessment. Hence, the research on cellular mechanisms during the induction of skin sensitization as well as the development of animal-free test guidelines have gained much attention in the field of toxicology over the last decades. In general, omics techniques were already applied in research on alternative methods for skin sensitization. Transcriptomics, for example, were successfully deployed for the discrimination of contact allergens from non-sensitizers in DC models (Hooyberghs et al., 2008; Johansson et al., 2011; Lambrechts et al., 2011). Although the proteome maps the phenotype of the biological organism more accurately, only few studies applying proteomics to investigate cellular mechanisms in the context of contact allergy were published to date (Höper et al., 2017; Koppes et al., 2017). Our group conducted a preceding study in human MoDCs to reveal differences in the cellular proteome after treatment with the metal contact allergen nickel *versus* the bacterial endotoxin LPS and found significant differences between the two treatments (Höper et al., 2021). Ni-treatment induced metabolic reprogramming, a pronounced Nrf2-mediated stress response, hypoxia as well as cholesterol depletion in MoDCs, whereas LPS-treated MoDCs displayed interferon signaling additionally to metabolic reprogramming and Nrf2 activation (Höper et al., 2021). Now, we aimed at screening multiple allergens to broaden the proteomic understanding of contact allergy. For this purpose, we selected THP-1 cells as surrogate model for DCs, as cell lines are better suited for screenings of broad sets of chemicals. Nevertheless, critical discussions on suitable cell models are inevitable in toxicology. Even though THP-1 cells are the selected cell model in the validated h-CLAT assay, they have been questioned due to their monocytic character and leukemia background.

For quantification of the proteomic data, we performed SILAC and LFQ, both of which are common approaches. LFQ can be applied to any kind of experimental setup and moreover was used for our preceding MoDC study. SILAC was selected as it is well-known for its high

reproducibility and precision (Li et al., 2012). Overall, both quantification strategies delivered comparable results in terms of affected pathways. Yet, more regulated proteins and pathways were identified based on SILAC data. Both techniques have their justification, but for cell lines SILAC is preferable, as it is easier to handle, requires substantial less measuring time at the mass spectrometer, minimizes measuring bias due to multiplexing and moreover, led to more detailed mechanistic insights due to the higher number of proteins found regulated. Thus, we recommend to use SILAC quantification when working with cell lines. Alternatively, chemical labeling like tandem mass tags (TMT) can be applied, which allows multiplexing of up to 16 samples and can be applied to any kind of sample as LFQ (Stepath et al., 2020; Wang et al., 2020).

4.2. Contact allergen-exposed THP-1 cells undergo pronounced metabolic shifts

Exposure of THP-1 cells to electrophils, such as contact allergens, results in a distinct cellular stress response that is largely mediated by Nrf2. Earlier *in vivo* studies with contact allergens have already suggested a substantial role of Nrf2 during skin sensitization (El Ali et al., 2013). Enzymes like NQO1, SOD2, glutathione s-transferases, heme oxygenase or catalase have been reported to be induced in allergen-treated THP-1 cells and DCs in the past (Lewis et al., 2006; Ade et al., 2009; Mussotter et al., 2016; Höper et al., 2021). Nrf2-mediated stress response can thus be considered a hallmark in DCs during skin sensitization. The central role of Nrf2 was also confirmed in keratinocytes, which led to the development of the KeratinoSens™ assay that has become an official OECD test guideline (OECD, 2018). Due to the power of proteomics, we are the first to report >40 regulated proteins upon contact allergen treatment linked to Nrf2-mediated stress response (Fig. 2C). We therefore recommend to use an additional Nrf2-related readout directly in DCs or DC surrogates.

In an antecedent multi-omics study, we already found evidence for metabolic reprogramming in THP-1 cells after treatment with the extreme skin sensitizer DNCB. The metabolome of DNCB-exposed cells was highly affected, pointing towards upregulation of glycolysis, TCA cycle and lipid synthesis (Mussotter et al., 2018). The current study confirms and expands these findings. Several metabolic pathways like TCA cycle, pentose phosphate pathway and oxidative phosphorylation were induced after treatment with all allergens investigated. In DCs, metabolic reprogramming was found to be crucial to support cellular activation following exposure to danger signals (Krawczyk et al., 2010). This metabolic adaption is typically characterized by upregulation of glycolysis and pentose phosphate pathway (PPP) with simultaneous downregulation of OXPHOS. DC activation *via* TLR massively increases aerobic glycolysis to a similar level as observed in cancer cells that display the typical Warburg effect (Kelly and O'Neill, 2015). The rapid metabolic switch supports maturation of the cells to enable migration to the draining lymph nodes and thereby ultimately enables immunological signaling as well as the induction of a systemic immune response. Induction of glycolytic proteins in contact allergen-exposed DCs was already reported in mouse bone marrow-derived DCs as well as in human MoDCs (Mussotter et al., 2016; Höper et al., 2021). Compared to the here investigated THP-1 cells, metabolic reprogramming in MoDCs was far less pronounced on proteome level (Höper et al., 2021). Elucidation of the underlying cellular mechanisms is complex and cannot be resolved using proteomics only. We speculate that the more pronounced metabolic activation of the THP-1 cells can partly be attributed to their cancer background (Warburg effect). Furthermore, the potency of a stimuli determines the degree of metabolic reprogramming both in DCs and monocytes (Lachmandas et al., 2016; Guak et al., 2018). Thus differences in metabolic shift can also be induced by different stimulatory potency of the contact allergens in different cells types.

Downstream of glycolysis, glycolytic products are fed into the TCA cycle, which was an activated metabolic pathway in the here investigated THP-1 cells. It has been shown that LPS-activated DCs rapidly upregulate glycolysis to increase the production of citrate *via* the TCA cycle (Everts et al., 2014). Citrate, which is transported to the cytosol to serve as a precursor for fatty acid and cholesterol biosynthesis, is required for maturation, involving restructuring of the plasma membrane. Our study confirms that most enzymes of the TCA cycle are upregulated after treatment of THP-1 cells with contact allergens (Fig. 2C). This is further supported by the upregulation of the PPP, which we also observed. Upregulation of PPP was also found in THP-1 cells treated with the sensitizer 2-hydroxyethylmethacrylate (Samuelsen et al., 2019). Importantly, the PPP supplies the cells with the reducing equivalent NADPH that is needed for fatty acid and cholesterol synthesis.

Interestingly, in the last ten years, it has become clear that the TCA cycle is not only important to deliver precursors for several synthesis routes but also is able to control various biological processes, including regulating cellular immunity. Since biological diseases and functions linked to inflammation were found to be upregulated in allergen-treated THP-1 cells, we suggest that the pronounced induction of the enzymes in the TCA cycle strongly supports a proinflammatory phenotype of the cells by providing respective metabolites. Citrate, for instance, has been shown to play an important role in key inflammatory pathways being relevant for macrophages as well as for DCs (Williams and O'Neill, 2018). Citrate is essential for the production of proinflammatory signaling molecules, including ROS and prostaglandin E2 (Infantino et al., 2014). Prostaglandin E2 is mandatory for the synthesis of pro-IL-1β after exposure of macrophages to LPS (Zasłona et al., 2017), and IL-1β was shown to play a major role during mediation of ACD (Yeung et al., 2021). Moreover, high levels of citrate and acetyl-CoA were shown to increase the expression of glycolytic enzymes in tumor cells (Lee et al., 2014).

Of all TCA cycle enzymes detected in this study, the only enzyme downregulated was succinate dehydrogenase, pointing towards a high succinate demand in the activated cells. Succinate is known to act as a proinflammatory signal in immune cells (Rubic et al., 2008; Tannahill et al., 2013). Furthermore, succinate was shown to enhance immunological signaling in DCs (Rubic et al., 2008) and to stabilize HIF-1α in the cytosol, thereby inducing genes like IL-1β important for glycolysis, inflammation and inflammasome activation (Tannahill et al., 2013; Li et al., 2016). Another potential fate of succinate could be the succinylation of lysine residues. Lysine succinylation can directly affect cellular metabolism by increasing enzyme activity of enzymes involved in glycolysis and TCA cycle (Park et al., 2013). Mitochondrial succinate can leak from dysfunctional mitochondria, and especially macrophages were shown to secrete succinate under inflammatory conditions (Littlewood-Evans et al., 2016). Extracellular succinate binds to its receptor SUCNR1 (succinate receptor 1) expressed on the plasma membrane of immune cells including DCs (Rubic et al., 2008; Littlewood-Evans et al., 2016), which is considered an immunological danger signal. Furthermore, succinate stimulates cell migration in a chemokine-like manner and enhances antigen-presentation to T cells as reported by Rubic et al. (2008). Indeed, *Suncr1*-deficient mice did not show elevated T cell activation after re-exposure of pre-sensitized mice to the contact allergen oxazolone (Rubić-Schneider et al., 2017).

To further elucidate the fate of TCA cycle metabolites in contact allergen-treated THP-1 cells, the proteomic data presented here should be complemented by a metabolomics experiment. In addition, mitochondrial respiration and glycolysis can for example be tracked using the seahorse analyzer. A metabolic flux analysis using isotope-labeled glucose or glutamine could reveal whether the disrupted TCA cycle that was described for LPS-treated macrophages and DCs (Everts et al., 2014; Galván-Peña and O'Neill, 2014) is also featured in THP-1 cells. Furthermore, inhibition of selected enzymes of the TCA cycle and analysis of downstream effects can be employed to support the proteomics data.

4.3. Affected pathways rather than single proteins are suitable for the comparative investigation of skin sensitization in THP-1 cells and MoDCs

One of our aims was to elucidate whether THP-1 cells are an appropriate surrogate to study proteomic changes during skin sensitization in DCs. Thus, we compared the effects uncovered here with effects observed in our previous study with MoDCs (Höper et al., 2021). We found that the overlap of regulated proteins was low between the two cell models (Supplementary Fig. 5). Based on the small overlap between the two cell systems on protein level, THP-1 cells should be considered a limited model for DCs. However, on enrichment level (pathways, diseases and functions) we obtained comparable results.

Exposure of DCs with contact allergens alters a broad range of proteins that orchestrate the complex immune response induced in the cells, eventually enabling presentation of the antigen to T cells. For T cells, antigen-specificity is well known (Chaplin, 2010) and specific T cell receptor repertoires were described for metal- as well as for chemical-induced allergy (Curato et al., 2022; Riedel et al., 2022). However, DCs are able to recognize, process and present a large range of antigens and thereby induce the antigen-specific immune response. Depending on the DC population, route of antigen uptake and the antigen itself, activation and maturation of DCs may vary and is not considered antigen-specific (Kamphorst et al., 2010; Alloatti et al., 2016). Due to this lack in specificity, it seems unlikely that specific protein biomarkers for skin sensitization can be identified in DCs. Thus, the use of predictive signatures seems more promising. Johansson et al. (2011) suggested a gene signature for the prediction of skin sensitizing chemicals *in vitro*. It is commonly known that the overlap between gene regulation and altered protein levels is not necessarily high. Yet, the integrative application of transcriptomic and proteomic data may support the identification of biomarkers, as it helps to uncover transcriptionally active mRNAs during the complex course of skin sensitization. We compared the GARD assay mRNA signature to regulated proteins in THP-1 cells after treatment with contact allergens, revealing 32 matching regulated proteins (Fig. 3A, SILAC). Among those, we found proteins linked to oxidative stress response like NQO1 and GSR, further underlining Nrf2-regulated pathways as hallmark during sensitization to exogenous chemicals. Also, proteins related to the cholesterol biosynthesis like HMGCS1 and CYP51A1 were regulated on mRNA level in MUTZ-3 cells as well as on protein level in THP-1 cells and MoDCs. Yet, directionality of protein regulation was contrary. These findings underline the evidence that cholesterol biosynthesis plays a pivotal role in allergen-treated DCs. However, due to equivocal regulation of proteins, this pathway has to be investigated further to assess its suitability as potential hallmark for skin sensitization. Notably, Lindberg et al. (2020) conducted a proteomics study in MUTZ-3 cells combined with the GARD assay to assess the skin sensitizing potential of glyphosate and its formulations. Here, 3 proteins were successfully matched to the predictive GARD signature and these proteins were also involved in cholesterol biosynthesis. Overall, we believe that the establishment of a proteomic signature of specific proteins and triggered cellular pathways might be more conducive than the search for individual biomarkers. Yet, a pathway-signature has to be chosen carefully to securely predict contact allergens based on proteomic data.

To be able to assess the suitability of a proteomic signature for the prediction of contact sensitizers in more depth, a larger set of contact sensitizers of different potency as well as irritants and non-allergenic chemicals should be analyzed to withdraw profound information for both cell systems, THP-1 cells and MoDCs, as the classification of allergens, irritants and non-allergenic chemicals is critical for proper risk assessment. The inclusion of irritants and non-allergens would thus increase the predictive power of the signature, as unspecific pathways can be identified and removed from the set of signature pathways. Furthermore, data from untargeted proteomic analyses could be used to develop a targeted proteomic method for routine testing of identified biomarkers and biomarker signatures. Moreover, THP-1 cells should be discussed more critically in the future when used as a tool for predicting contact allergens based on proteomic studies. Further proteomics studies should be conducted to investigate if THP-1 cells, differentiated into a DC-like phenotype before contact allergen treatment, resemble DCs more closely. Furthermore, a comparative proteomic study comparing THP-1 and MUTZ-3 cells could provide information on the suitability of these cell lines for the proteomic investigation of skin sensitization.

5. Conclusion

Overall, our study underlines the power of proteomics to unravel toxicity mechanisms. When comparing the two different proteomics approaches applied here, SILAC and LFQ, certainly both have their justification. However, when working with cell lines, SILAC should be preferred as it delivers more robust data and yields a higher number of regulated proteins.

The four allergens BQ, DNCB, NBB and Ni overall showed comparable responses in THP-1 cells, which underwent profound metabolic reprogramming that was accompanied by pronounced induction of proteins of the Nrf2 oxidative stress response pathway. The TCA cycle seems to play a central role and might be connected to the proinflammatory response. Compared to Ni-treated MoDCs, similar IPA diseases and functions as well as pathways were triggered in THP-1 cells but the overlap on the protein level was rather low. When aiming to improve existing *in vitro* assays by proteomic signatures, one should therefore focus on proteins that are regulated by allergens in both, THP-1 cells and primary MoDCs. This includes proteins of the Nrf2 pathway along with proteins from glycolytic and lipid metabolism. For the elucidation of cellular modes of action, primary cells seem to be superior, as THP-1 cells were reacting unidimensional and showed a much less complex network of induced IPA pathways compared to MoDCs.

Funding

The authors acknowledge financial support from BfR. The work was funded *via* a BfR-internal grant (SFP 1322-470), which is gratefully appreciated.

CRediT authorship contribution statement

T. Höper: Conceptualization, Investigation, Methodology, Project administration, Data curation, Formal analysis, Writing – original draft, Writing – review & editing. **I. Karkossa**: Methodology, Data curation, Formal analysis, Software, Visualization, Writing – original draft, Writing – review & editing. **V. I. Dumit**: Conceptualization, Supervision, Writing – review & editing. **M. von Bergen**: Conceptualization, Resources, Writing – review & editing. **K. Schubert**: Conceptualization, Writing – review & editing. **A. Haase**: Conceptualization, Funding acquisition, Project administration, Resources, Supervision, Writing – review & editing.

Declaration of Competing Interest

The authors declare that the research was conducted in the absence of any commercial or financial relationships that could be construed as a potential conflict of interest.

Data availability

The dataset presented in this study can be found online in the PRIDE repository (Perez-Riverol et al., 2019) with the dataset identifier PXD031017. A full list of all proteins, including the protein names and accessions as well as Log2(FCs) and adjusted p-values can be found in the article supplementary material.

Acknowledgments

The authors would like to thank all institutions and the UFZ-funded ProMetheus platform for proteomics and metabolomics for the support of this project.

Appendix A. Supplementary data

Supplementary data to this article can be found online at https://doi.org/10.1016/j.taap.2023.116650.

References

Ade, N., Leon, F., Pallardy, M., Peiffer, J.L., Kerdine-Romer, S., Tissier, M.H., Bonnet, P. A., Fabre, I., Ourlin, J.C., 2009. HMOX1 and NQO1 genes are upregulated in response to contact sensitizers in dendritic cells and THP-1 cell line: role of the Keap1/Nrf2 pathway. Toxicol. Sci. 107, 451–460.

Adrian, A.D., Cole, A., 2018. xlsx: Read, Write, Format Excel 2007 and Excel 97/2000/XP/2003 Files. R Package Version 0.6.1. https://CRAN.R-project.org/package=xlsx.

Alloatti, A., Kotsias, F., Magalhaes, J.G., Amigorena, S., 2016. Dendritic cell maturation and cross-presentation: timing matters! Immunol. Rev. 272, 97–108.

Ananda, M., 2019. splitstackshape: Stack and Reshape Datasets After Splitting Concatenated Values. R Package Version 1.4.8. https://CRAN.R-project.org/package=splitstackshape.

Andrej-Nikolai, S., 2018. qpcR: Modelling and Analysis of Real-Time PCR Data. R Package Version 1.4–1. https://CRAN.R-project.org/package=qpcR.

Ashikaga, T., Yoshida, Y., Hirota, M., Yoneyama, K., Itagaki, H., Sakaguchi, H., Miyazawa, M., Ito, Y., Suzuki, H., Toyoda, H., 2006. Development of an in vitro skin sensitization test using human cell lines: the human cell line activation test (h-CLAT). I. Optimization of the h-CLAT protocol. Toxicol. in Vitro 20.

Ashikaga, T., Sakaguchi, H., Sono, S., Kosaka, N., Ishikawa, M., Nukada, Y., Miyazawa, M., Ito, Y., Nishiyama, N., Itagaki, H., 2010. A comparative evaluation of in vitro skin sensitisation tests: the human cell-line activation test (h-CLAT) versus the local lymph node assay (LLNA). Altern. Lab. Anim 38, 275–284.

Chaplin, D.D., 2010. Overview of the immune response. J. Allergy Clin. Immunol. 125, S3–23.

Cox, J., Hein, M.Y., Luber, C.A., Paron, I., Nagaraj, N., Mann, M., 2014. Accurate proteome-wide label-free quantification by delayed normalization and maximal peptide ratio extraction, termed MaxLFQ. Mol. Cell. Proteomics 13, 2513–2526.

Curato, C., Aparicio-Soto, M., Riedel, F., Wehl, I., Basaran, A., Abbas, A., Thierse, H.J., Luch, A., Siewert, K., 2022. Frequencies and TCR repertoires of human 2,4,6-Trinitrobenzenesulfonic acid-specific T cells. Front. Toxicol. 4, 827109.

Dhingra, N., Shemer, A., Correa da Rosa, J., Rozenblit, M., Fuentes-Duculan, J., Gittler, J. K., Finney, R., Czarnowicki, T., Zheng, X., Xu, H., Estrada, Y.D., Cardinale, I., Suárez-Fariñas, M., Krueger, J.G., Guttman-Yassky, E., 2014. Molecular profiling of contact dermatitis skin identifies allergen-dependent differences in immune response. J. Allergy Clin. Immunol. 134, 362–372.

EC, 2009. Regulation (EC) no 1223/2009 of the European Parliament and of the council of 30 November 2009 on cosmetic products. Off. J. Eur. Union L342, 59–209.

El Ali, Z., Gerbeix, C., Hemon, P., Esser, P.R., Martin, S.F., Pallardy, M., Kerdine-Römer, S., 2013. Allergic skin inflammation induced by chemical sensitizers is controlled by the transcription factor Nrf2. Toxicol. Sci. 134, 39–48.

Emter, R., Ellis, G., Natsch, A., 2010. Performance of a novel keratinocyte-based reporter cell line to screen skin sensitizers in vitro. Toxicol. Appl. Pharmacol. 245, 281–290.

Everts, B., Amiel, E., Huang, S.C., Smith, A.M., Chang, C.H., Lam, W.Y., Redmann, V., Freitas, T.C., Blagih, J., van der Windt, G.J., Artyomov, M.N., Jones, R.G., Pearce, E. L., Pearce, E.J., 2014. TLR-driven early glycolytic reprogramming via the kinases TBK1-IKKvarepsilon supports the anabolic demands of dendritic cell activation. Nat. Immunol. 15, 323–332.

Fabian, E., Vogel, D., Blatz, V., Ramirez, T., Kolle, S., Eltze, T., van Ravenzwaay, B., Oesch, F., Landsiedel, R., 2013. Xenobiotic metabolizing enzyme activities in cells used for testing skin sensitization in vitro. Arch. Toxicol. 87, 1683–1696.

Galván-Peña, S., O'Neill, L.A.J., 2014. Metabolic reprograming in macrophage polarization. Front. Immunol. 5.

Gerberick, G.F., Vassallo, J.D., Bailey, R.E., Chaney, J.G., Morrall, S.W., Lepoittevin, J.P., 2004. Development of a peptide reactivity assay for screening contact allergens. Toxicol. Sci. 81, 332–343.

Gerberick, G.F., Ryan, C.A., Kern, P.S., Schlatter, H., Dearman, R.J., Kimber, I., Patlewicz, G.Y., Basketter, D.A., 2005. Compilation of historical local lymph node data for evaluation of skin sensitization alternative methods. Dermatitis 16, 157–202.

Gerberick, G.F., Vassallo, J.D., Foertsch, L.M., Price, B.B., Chaney, J.G., Lepoittevin, J.P., 2007. Quantification of chemical peptide reactivity for screening contact allergens: a classification tree model approach. Toxicol. Sci. 97, 417–427.

Gu, Z., 2014. Circlize implements and enhances circular visualization in R. Bioinformatics 30, 2811–2812.

Guak, H., Al Habyan, S., Ma, E.H., Aldossary, H., Al-Masri, M., Won, S.Y., Ying, T., Fixman, E.D., Jones, R.G., McCaffrey, L.M., Krawczyk, C.M., 2018. Glycolytic metabolism is essential for CCR7 oligomerization and dendritic cell migration. Nat. Commun. 9, 2463.

Guedes, S., Neves, B., Vitorino, R., Domingues, R., Cruz, M.T., Domingues, P., 2016. Contact dermatitis: in pursuit of sensitizer's molecular targets through proteomics. Arch. Toxicol. 1–15.

Hadley, W., 2016. ggplot2: Elegant Graphics for Data Analysis. Springer-Verlag, New York.

Hadley, W., Jennifer, B., 2019. readxl: Read Excel Files. R Package Version 1.3.1. https://CRAN.R-project.org/package=readxl.

Hadley, W., Lionel, H., 2019. tidyr: Tidy Messy Data. R Package Version 1.0.0. https://CRAN.R-project.org/package=tidyr.

Hooyberghs, J., Schoeters, E., Lambrechts, N., Nelissen, I., Witters, H., Schoeters, G., Van Den Heuvel, R., 2008. A cell-based in vitro alternative to identify skin sensitizers by gene expression. Toxicol. Appl. Pharmacol. 231, 103–111.

Höper, T., Mussotter, F., Haase, A., Luch, A., Tralau, T., 2017. Application of proteomics in the elucidation of chemical-mediated allergic contact dermatitis. Toxicol. Res. 6, 595–610.

Höper, T., Siewert, K., Dumit, V.I., von Bergen, M., Schubert, K., Haase, A., 2021. The contact allergen NiSO4 triggers a distinct molecular response in primary human dendritic cells compared to bacterial LPS. Front. Immunol. 12.

Infantino, V., Iacobazzi, V., Menga, A., Avantaggiati, M.L., Palmieri, F., 2014. A key role of the mitochondrial citrate carrier (SLC25A1) in TNFα- and IFNγ-triggered inflammation. Biochim. Biophys. Acta (BBA) - Gene Regul. Mech. 1839, 1217–1225.

Jan, G., 2019. calibrate: Calibration of Scatterplot and Biplot Axes. R Package Version 1.7.5. https://CRAN.R-project.org/package=calibrate.

Jaworska, J.S., Natsch, A., Ryan, C., Strickland, J., Ashikaga, T., Miyazawa, M., 2015. Bayesian integrated testing strategy (ITS) for skin sensitization potency assessment: a decision support system for quantitative weight of evidence and adaptive testing strategy. Arch. Toxicol. 89, 2355–2383.

Johansson, H., Lindstedt, M., Albrekt, A.-S., Borrebaeck, C.A., 2011. A genomic biomarker signature can predict skin sensitizers using a cell-based in vitro alternative to animal tests. BMC Genomics 12, 399.

Johansson, H., Albrekt, A.S., Borrebaeck, C.A., Lindstedt, M., 2013. The GARD assay for assessment of chemical skin sensitizers. Toxicol. in Vitro 27, 1163–1169.

Kamphorst, A.O., Guermonprez, P., Dudziak, D., Nussenzweig, M.C., 2010. Route of antigen uptake differentially impacts presentation by dendritic cells and activated monocytes. J. Immunol. 185, 3426.

Kelly, B., O'Neill, L.A., 2015. Metabolic reprogramming in macrophages and dendritic cells in innate immunity. Cell Res. 25, 771–784.

Kolde, R., 2019. pheatmap: Pretty Heatmaps [Online]. Available: https://CRAN.R-project.org/package=pheatmap [Accessed 26.04.2021].

Koppes, S.A., Engebretsen, K.A., Agner, T., Angelova-Fischer, I., Berents, T., Brandner, J., Brans, R., Clausen, M.L., Hummler, E., Jakasa, I., Jurakic-Toncic, R., John, S.M., Khnykin, D., Molin, S., Holm, J.O., Suomela, S., Thierse, H.J., Kezic, S., Martin, S.F., Thyssen, J.P., 2017. Current knowledge on biomarkers for contact sensitization and allergic contact dermatitis. Contact Dermatitis 77, 1–16.

Krämer, A., Green, J., Pollard Jr., J., Tugendreich, S., 2013. Causal analysis approaches in ingenuity pathway analysis. Bioinformatics 30, 523–530.

Krawczyk, C.M., Holowka, T., Sun, J., Blagih, J., Amiel, E., DeBerardinis, R.J., Cross, J. R., Jung, E., Thompson, C.B., Jones, R.G., Pearce, E.J., 2010. Toll-like receptor-induced changes in glycolytic metabolism regulate dendritic cell activation. Blood 115, 4742–4749.

Lachmandas, E., Boutens, L., Ratter, J.M., Hijmans, A., Hooiveld, G.J., Joosten, L.A.B., Rodenburg, R.J., Fransen, J.A.M., Houtkooper, R.H., van Crevel, R., Netea, M.G., Stienstra, R., 2016. Microbial stimulation of different toll-like receptor signalling pathways induces diverse metabolic programmes in human monocytes. Nat. Microbiol. 2, 16246.

Lambrechts, N., Nelissen, I., Van Tendeloo, V., Witters, H., Van Den Heuvel, R., Hooyberghs, J., Schoeters, G., 2011. Functionality and specificity of gene markers for skin sensitization in dendritic cells. Toxicol. Lett. 203, 106–110.

Lee, J.V., Carrer, A., Shah, S., Snyder, N.W., Wei, S., Venneti, S., Worth, A.J., Yuan, Z.F., Lim, H.W., Liu, S., Jackson, E., Aiello, N.M., Haas, N.B., Rebbeck, T.R., Judkins, A., Won, K.J., Chodosh, L.A., Garcia, B.A., Stanger, B.Z., Feldman, M.D., Blair, I.A., Wellen, K.E., 2014. Akt-dependent metabolic reprogramming regulates tumor cell histone acetylation. Cell Metab. 20, 306–319.

Lefevre, M.-A., Nosbaum, A., Rozieres, A., Lenief, V., Mosnier, A., Cortial, A., Prieux, M., De Bernard, S., Nourikyan, J., Jouve, P.-E., Buffat, L., Hacard, F., Ferrier-Lebouedec, M.-C., Pralong, P., Dzviga, C., Herman, A., Baeck, M., Nicolas, J.-F., Vocanson, M., 2021. Unique molecular signatures typify skin inflammation induced by chemical allergens and irritants. Allergy 76, 3697–3712.

Lewis, J.B., Messer, R.L., McCloud, V.V., Lockwood, P.E., Hsu, S.D., Wataha, J.C., 2006. Ni(II) activates the Nrf2 signaling pathway in human monocytic cells. Biomaterials 27, 5348–5356.

Li, Z., Adams, R.M., Chourey, K., Hurst, G.B., Hettich, R.L., Pan, C., 2012. Systematic comparison of label-free, metabolic labeling, and isobaric chemical labeling for quantitative proteomics on LTQ Orbitrap Velos. J. Proteome Res. 11, 1582–1590.

Li, Y., Zheng, J.Y., Liu, J.Q., Yang, J., Liu, Y., Wang, C., Ma, X.N., Liu, B.L., Xin, G.Z., Liu, L.F., 2016. Succinate/NLRP3 inflammasome induces synovial fibroblast activation: therapeutical effects of clematichinenoside AR on arthritis. Front. Immunol. 7, 532.

Lindberg, T., de Ávila, R.I., Zeller, K.S., Levander, F., Eriksson, D., Chawade, A., Lindstedt, M., 2020. An integrated transcriptomic- and proteomic-based approach to evaluate the human skin sensitization potential of glyphosate and its commercial agrochemical formulations. J. Proteome 217, 103647.

Littlewood-Evans, A., Sarret, S., Apfel, V., Loesle, P., Dawson, J., Zhang, J., Muller, A., Tigani, B., Kneuer, R., Patel, S., Valeaux, S., Gommermann, N., Rubic-Schneider, T., Junt, T., Carballido, J.M., 2016. GPR91 senses extracellular succinate released from

inflammatory macrophages and exacerbates rheumatoid arthritis. J. Exp. Med. 213, 1655–1662.
Martin, S.F., Esser, P.R., Weber, F.C., Jakob, T., Freudenberg, M.A., Schmidt, M., Goebeler, M., 2011. Mechanisms of chemical-induced innate immunity in allergic contact dermatitis. Allergy 66, 1152–1163.
Mussotter, F., Tomm, J.M., El Ali, Z., Pallardy, M., Kerdine-Romer, S., Gotz, M., von Bergen, M., Haase, A., Luch, A., 2016. Proteomics analysis of dendritic cell activation by contact allergens reveals possible biomarkers regulated by Nrf2. Toxicol. Appl. Pharmacol. 313, 170–179.
Mussotter, F., Potratz, S., Budczies, J., Luch, A., Haase, A., 2018. A multi-omics analysis reveals metabolic reprogramming in THP-1 cells upon treatment with the contact allergen DNCB. Toxicol. Appl. Pharmacol. 340, 21–29.
Nan, X., 2018. ggsci: Scientific Journal and Sci-Fi Themed Color Palettes for 'ggplot2'. R Package Version 2.9. https://CRAN.R-project.org/package=ggsci.
Nukada, Y., Miyazawa, M., Kazutoshi, S., Sakaguchi, H., Nishiyama, N., 2013. Data integration of non-animal tests for the development of a test battery to predict the skin sensitizing potential and potency of chemicals. Toxicol. in Vitro 27, 609–618.
OECD, 2014. The Adverse Outcome Pathway for Skin Sensitisation Initiated by Covalent Binding to Proteins.
OECD, 2018. Test No. 442D: In Vitro Skin Sensitisation.
OECD, 2021. Guideline No. 497: Defined Approaches on Skin Sensitisation.
OECD, 2022a. Test No. 442C: In Chemico Skin Sensitisation.
OECD, 2022b. Test No. 442D: In Vitro Skin Sensitisation.
OECD, 2022c. Test No. 442E: In Vitro Skin Sensitisation.
Oesch, F., Fabian, E., Guth, K., Landsiedel, R., 2014. Xenobiotic-metabolizing enzymes in the skin of rat, mouse, pig, guinea pig, man, and in human skin models. Arch. Toxicol. 88, 2135–2190.
Oosterhaven, J.A.F., Uter, W., Aberer, W., Armario-Hita, J.C., Ballmer-Weber, B.K., Bauer, A., Czarnecka-Operacz, M., Elsner, P., García-Gavín, J., Giménez-Arnau, A. M., John, S.M., Kręcisz, B., Mahler, V., Rustemeyer, T., Sadowska-Przytocka, A., Sánchez-Pérez, J., Simon, D., Valiukevičienė, S., Weisshaar, E., Schuttelaar, M.L.A., 2019. European surveillance system on contact allergies (ESSCA): contact allergies in relation to body sites in patients with allergic contact dermatitis. Contact Dermatitis 80, 263–272.
Park, J., Chen, Y., Tishkoff, Daniel X., Peng, C., Tan, M., Dai, L., Xie, Z., Zhang, Y., Zwaans, Bernadette M.M., Skinner, Mary E., Lombard, David B., Zhao, Y., 2013. SIRT5-mediated lysine desuccinylation impacts diverse metabolic pathways. Mol. Cell 50, 919–930.
Parkinson, E., Boyd, P., Aleksic, M., Cubberley, R., O'Connor, D., Skipp, P., 2014. Stable isotope labeling method for the investigation of protein haptenation by electrophilic skin sensitizers. Toxicol. Sci. 142, 239–249.
Parkinson, E., Aleksic, M., Cubberley, R., Kaur-Atwal, G., Vissers, J.P.C., Skipp, P., 2018. Determination of protein haptenation by chemical sensitizers within the complexity of the human skin proteome. Toxicol. Sci. 162, 429–438.
Parkinson, E., Aleksic, M., Kukic, P., Bailey, A., Cubberley, R., Skipp, P., 2020. Proteomic analysis of the cellular response to a potent sensitiser unveils the dynamics of haptenation in living cells. Toxicology 445, 152603.
Perez-Riverol, Y., Csordas, A., Bai, J., Bernal-Llinares, M., Hewapathirana, S., Kundu, D. J., Inuganti, A., Griss, J., Mayer, G., Eisenacher, M., Perez, E., Uszkoreit, J., Pfeuffer, J., Sachsenberg, T., Yilmaz, S., Tiwary, S., Cox, J., Audain, E., Walzer, M., Jarnuczak, A.F., Ternent, T., Brazma, A., Vizcaino, J.A., 2019. The PRIDE database and related tools and resources in 2019: improving support for quantification data. Nucleic Acids Res. 47, D442–D450.
Qiagen. Ingenuity Pathway Analysis [Online]. Available: https://www.qiagenbioinformatics.com/products/ingenuity-pathway-analysis/.
Reisinger, K., Hoffmann, S., Alépée, N., Ashikaga, T., Barroso, J., Elcombe, C., Gellatly, N., Galbiati, V., Gibbs, S., Groux, H., Hibatallah, J., Keller, D., Kern, P., Klaric, M., Kolle, S., Kuehnl, J., Lambrechts, N., Lindstedt, M., Millet, M., Martinozzi-Teissier, S., Natsch, A., Petersohn, D., Pike, I., Sakaguchi, H., Schepky, A., Tailhardat, M., Templier, M., van Vliet, E., Maxwell, G., 2015. Systematic evaluation of non-animal test methods for skin sensitisation safety assessment. Toxicol. in Vitro 29, 259–270.
Riedel, F., Aparicio-Soto, M., Curato, C., Münch, L., Abbas, A., Thierse, H.J., Peitsch, W. K., Luch, A., Siewert, K., 2022. Unique and common TCR repertoire features of Ni(2+) -, Co(2+) -, and Pd(2+) -specific human CD154 +CD4+ T cells. Allergy 78, 270–282.
Rohart, F., Gautier, B., Singh, A., Le Cao, K.A., 2017. mixOmics: an R package for 'omics feature selection and multiple data integration. PLoS Comput. Biol. 13, e1005752.
Rubic, T., Lametschwandtner, G., Jost, S., Hinteregger, S., Kund, J., Carballido-Perrig, N., Schwärzler, C., Junt, T., Voshol, H., Meingassner, J.G., Mao, X., Werner, G., Rot, A., Carballido, J.M., 2008. Triggering the succinate receptor GPR91 on dendritic cells enhances immunity. Nat. Immunol. 9, 1261–1269.
Rubić-Schneider, T., Carballido-Perrig, N., Regairaz, C., Raad, L., Jost, S., Rauld, C., Christen, B., Wieczorek, G., Kreutzer, R., Dawson, J., Lametschwandner, G., Littlewood-Evans, A., Carballido, J.M., 2017. GPR91 deficiency exacerbates allergic contact dermatitis while reducing arthritic disease in mice. Allergy 72, 444–452.
Sakai, R., 2015. dendsort: Modular Leaf Ordering Methods for Dendrogram Nodes. R Package Version 0.3. 3.
Samuelsen, J.T., Michelsen, V.B., Bruun, J.A., Dahl, J.E., Jensen, E., Ortengren, U., 2019. The dental monomer HEMA causes proteome changes in human THP-1 monocytes. J. Biomed. Mater. Res. A 107, 851–859.
Stepath, M., Zülch, B., Maghnouj, A., Schork, K., Turewicz, M., Eisenacher, M., Hahn, S., Sitek, B., Bracht, T., 2020. Systematic comparison of label-free, SILAC, and TMT techniques to study early adaption toward inhibition of EGFR signaling in the colorectal cancer cell line DiFi. J. Proteome Res. 19, 926–937.
Stephen, T., 2019. Tmisc: Turner Miscellaneous. R Package Version 0.1.22. https://CRAN.R-project.org/package=Tmisc.
Takenouchi, O., Miyazawa, M., Saito, K., Ashikaga, T., Sakaguchi, H., 2013. Predictive performance of the human cell line activation test (h-CLAT) for lipophilic chemicals with high octanol-water partition coefficients. J. Toxicol. Sci. 38, 599–609.
Tannahill, G.M., Curtis, A.M., Adamik, J., Palsson-McDermott, E.M., McGettrick, A.F., Goel, G., Frezza, C., Bernard, N.J., Kelly, B., Foley, N.H., Zheng, L., Gardet, A., Tong, Z., Jany, S.S., Corr, S.C., Haneklaus, M., Caffrey, B.E., Pierce, K., Walmsley, S., Beasley, F.C., Cummins, E., Nizet, V., Whyte, M., Taylor, C.T., Lin, H., Masters, S.L., Gottlieb, E., Kelly, V.P., Clish, C., Auron, P.E., Xavier, R.J., O'Neill, L.A.J., 2013. Succinate is an inflammatory signal that induces IL-1β through HIF-1α. Nature 496, 238–242.
Wang, Z., Karkossa, I., Großkopf, H., Rolle-Kampczyk, U., Hackermüller, J., von Bergen, M., Schubert, K., 2020. Comparison of quantitation methods in proteomics to define relevant toxicological information on AhR activation of HepG2 cells by BaP. Toxicology 152652.
Wickham, H., 2007. Reshaping data with thereshapePackage. J. Stat. Softw. 21.
Wickham, H., 2011. The split-apply-combine strategy for data analysis. J. Stat. Softw. 40.
Williams, N.C., O'Neill, L.A.J., 2018. A role for the Krebs cycle intermediate citrate in metabolic reprogramming in innate immunity and inflammation. Front. Immunol. 9, 141.
Yeung, K., Mraz, V., Geisler, C., Skov, L., Bonefeld, C.M., 2021. The role of interleukin-1β in the immune response to contact allergens. Contact Dermatitis 85, 387–397.
Zasłona, Z., Pålsson-McDermott, E.M., Menon, D., Haneklaus, M., Flis, E., Prendeville, H., Corcoran, S.E., Peters-Golden, M., O'Neill, L.A.J., 2017. The induction of pro-IL-1β by lipopolysaccharide requires endogenous prostaglandin E(2) production. J. Immunol. 198, 3558–3564.
Zhang, X., Smits, A.H., van Tilburg, G.B., Ovaa, H., Huber, W., Vermeulen, M., 2018. Proteome-wide identification of ubiquitin interactions using UbIA-MS. Nat. Protoc. 13, 530–550.